A R C H I V E S O F M E T A L L U R G Y A N D M A T E R I A L S
Volume 59 2014 Issue 1
DOI: 10.2478/amm-2014-0003

R. BIDULSKÝ[*,**], J. BIDULSKÁ[**], M. ACTIS GRANDE[*]

ANALYSIS OF DENSIFICATION PROCESS AND STRUCTURE OF PM Al-Mg-Si-Cu-Fe AND Al-Zn-Mg-Cu-Sn ALLOYS

ANALIZA PROCESU ZAGĘSZCZANIA I STRUKTURY SPIEKANYCH STOPÓW Al-Mg-Si-Cu-Fe I Al-Zn-Mg-Cu-Sn

The paper is focused on the role of the pressing pressure on the densification behaviour of PM aluminium alloys. Commercially aluminium based powders Al-Mg-Si-Cu-Fe and Al-Zn-Mg-Cu-Sn were used as materials to be investigated. The apparent density of the powder mixes was determined according to MPIF St. 04. A set of cylinder test specimen 55×10×10 mm^3 was uniaxially pressed in a floating hardened steel die. Compaction pressures ranged from 50 MPa up to 700 MPa. Considering the densification of metal powders in uniaxial compaction, quantification of aluminium compaction behaviour was performed. The compressibility behaviour was evaluated, considering the effect on specimens, as well as on their microstructure.

The development of compressibility values with pressing pressure enables to characterize the effect of particles geometry and matrix plasticity on the compaction process.

Keywords: Powder Metallurgy, Aluminium Alloy, Compressibility, Microstructure

Przedmiotem pracy jest wpływ ciśnienia prasowania na zagęszczanie proszków stopów aluminium. Materiałem badanym były komercyjne proszki aluminium Al-Mg-Si-Cu-Fe I Al-Zn-Mg-Cu-Sn. Gęstość pozorną mieszanek proszków określono według MPIF St.04. Cylindryczne próbki 55×10×10 mm^3 ściskane były jednokierunkowo w samonastawnej matrycy z hartowanej stali. Nacisk wahał się od 50 MPa do 700 MPa. Biorąc pod uwagę zagęszczenie proszków metali w trakcie prasowania jednoosiowego, przeprowadzono kwantyfikację zagęszczania aluminium. Oceniono zachowanie ściśliwości biorąc pod uwagę wpływ na próbki, jak również na ich mikrostrukturę. Zestawienie wartości ściśliwości z ciśnieniem prasowania pozwala scharakteryzować wpływ geometrii cząstek i plastyczności matrycy na proces prasowania.

1. Introduction

Powder metallurgy (PM) is an advanced metal forming technique used to fabricate precision products in a near-net-shape form [1, 2]. Fundamental stages of this process include blending of powder, delivery of powder into the die (die filling); powder transfer (principally for multilevel components); powder compaction; ejection from the die; sintering; secondary operation (other plastic deformation processes, or heat treatment processes, and sizing). As a near net shape processes, it can produce components, typically of small size and of complex shape, with high precision at low cost level. The requirements on complex properties (i.e. high tensile strength with adequate plasticity and weight ratio) in automotive industry provide an increasing role for aluminium alloys also in the PM market. The car industry is the most lucrative market for PM aluminium alloys. These light weight materials are expected to replace iron and steel parts in automobiles in order to reduce weight, increase fuel efficiency and also reduce exhaust emission.

However, on the market, there are not many PM products available. The lack of commercially available 'press and sinter' aluminium alloys corresponds to a narrow range of mechanical properties [3]. Various consolidation routes are used for significantly enhancing mechanical properties, mainly deformation processes which have significant shear stress components: extrusion, sinterforging, uniaxial hot pressing, hot isostatic pressing; and non-conventional consolidation methods such as microwave sintering, field assisted sintering methods, and shockwave consolidation; as well as severe plastic deformation processes (SPD) [4].

In the PM area, SPD is a relatively new technological solution for achieving high strength [5-7]. However, significant improvements in basic material properties are not necessarily accompanied with comparable improvements in properties such as fatigue and wear resistance that depend more sensitively on highly localized defects [8-11] and the presence of microstructural inhomogeneities [12, 13]. Strain induced voids/porosity may fundamentally limit the enhancements that can be achieved in these properties. In order to precisely evaluate the powder behaviour, new approaches are necessary, including the investigation of powder behaviour, nano/micro technique for identification of microstructural inhomogeneities in PM materials [14-18], as well as mathematical and com-

[*] DEPARTMENT OF APPLIED SCIENCE AND TECHNOLOGY, POLITECNICO DI TORINO, ALESSANDRIA CAMPUS, VIALE T. MICHEL 5, 15121 ALESSANDRIA, ITALY
[**] DEPARTMENT OF METALS FORMING, FACULTY OF METALLURGY, TECHNICAL UNIVERSITY OF KOŠICE, VYSOKOŠKOLSKÁ 4, 04200 KOŠICE, SLOVAKIA

puter simulation [19-22], mainly in the description of densification behaviour after SPD process.

Despite the aforementioned processes and their mechanical properties enhanced, the rigid die compaction is still widely employed for the production of PM parts, mainly due to cost effectiveness reason. In order to fully evaluate the powder compressibility, the relationship between density or porosity and the applied pressure as well microstructure evolution during compaction are crucial steps for a complete knowledge of the first step of the traditional PM process.

2. Experimental conditions

Commercial ready-to-press aluminium based powders (ECKA Alumix 321 and ECKA Alumix 431) were used as materials to be investigated. The microstructures of basic powders are presented in Fig. 1 (Al-Mg-Si-Cu-Fe) and Fig. 2 (Al-Zn-Mg-Cu-Sn).

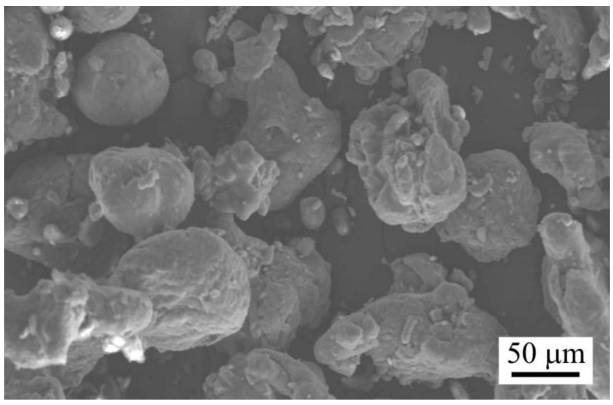

Fig. 1. The microstructure of the as-receive aluminium Al-Mg-Si-Cu-Fe powder

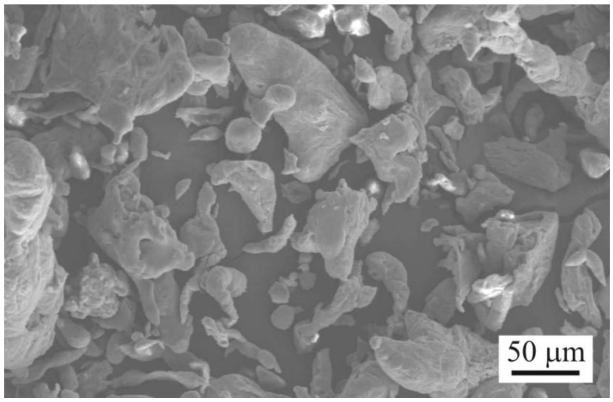

Fig. 2. The microstructure of the as-receive aluminium Al-Zn-Mg-Cu-Sn powder

Formulations of the tested alloys are presented in Table 1 (wt. %).

Particles size distribution, usually representing the mass percentage retained upon each of series of standard sieves of decreasing size and the percentage passed by the sieve of finest size, was carried out by sieve analyzer according to ISO 4497. The apparent density of powders was determined according to MPIF Standard 04. The tap density of powders was determined according to MPIF Standard 46. Specimens were obtained using a 2000 kN hydraulic press, applying different pressures from 50 MPa to 700 MPa. A set of cylinder test specimen 55×10×10 mm^3 was uniaxially pressed in a floating hardened steel die. The green compacts were weighed with an accuracy of ±0.001 g. The dimensions were measured with a micrometer calliper (±0.01 mm). The following compressibility equation [23-25] was used:

TABLE 1
Chemical compositions of investigated PM aluminium alloys

Alumix 321					
Al	**lubricant**	**Mg**	**Si**	**Cu**	**Fe**
balance	1.50	0.95	0.49	0.21	0.07
Alumix 431					
Al	**lubricant**	**Mg**	**Zn**	**Cu**	**Sn**
balance	1.56	2.6	5.8	1.7	0.23

$$P = P_0 \cdot \exp(-K \cdot p^n) \quad [\%] \tag{1}$$

where:

P [%], porosity achieved at an applied pressure p;

P_0 [%], apparent porosity calculated from the value of experimentally estimated apparent density:

$$P_0 = \left[1 - \frac{\rho_a}{\rho_{th}} \cdot 100\right] \quad [\%] \tag{2}$$

p [MPa], applied pressure;

K [-], a parameter related to particle morphology;

n [-], a parameter related to activity of powders to densification by the plastic deformation only.

Using the linear form of equation (1):

$$\ln\left[\ln\left(\frac{P_0}{P}\right)\right] = -\ln K + n \cdot \ln p \tag{3}$$

The parameters K and n can be calculated by linear regression analysis. A linear relationship between the parameters K and n was found and described in [24]:

$$\ln K = f(p): \quad \ln K = a - b \cdot n \tag{4}$$

where:

a=1.432;

b=7.6;

correlation coefficient r=0.9665.

3. Results

The measured characteristics of the as-received aluminium powders are presented in Table 2 and Table 3, where the particle size distribution of both investigated aluminium alloys are reported. It can be seen from the results that the largest fraction of particles for the investigated material is in range of 63 to 100 μm. Particle size distribution of investigated aluminium alloys are presented in Table 2 and Table 3.

TABLE 2
Particle size distribution of investigated Al-Mg-Si-Cu-Fe aluminium alloy

Size fraction [μm]	Fraction [%]	St. deviation
200-250	**1.4**	1.6
160-200	**7.3**	0.7
100-160	**28.7**	8.7
63-100	**48.8**	7.3
45-63	**8.8**	3.5
<45	**5**	5

TABLE 3
Particle size distribution of investigated Al-Zn-Mg-Cu-Sn aluminium alloy

Size fraction [μm]	Fraction [%]	St. deviation
200-250	**1**	1.4
160-200	**3.4**	0.9
100-160	**26.2**	8.3
63-100	**31.2**	8.5
45-63	**17.2**	5.3
<45	**21**	7.1

Variations in particle size distribution and consequently in the uniformity of powder mixes significantly influence the specimens' density and the mechanical properties including strength, wear and fatigue. Therefore, particle size distribution strongly affected apparent and tap density (Table 4). The finer Al-Zn-Mg-Cu-Sn alloy achieved three times higher tap density than Al-Mg-Si-Cu-Fe alloy. For example, the powders with a higher tap density generally have a lower sintered density than powders of similar size but different shape. The smaller the particles the greater the specific surface of the powder system is. Reference [26] suggested that this phenomenon increases the friction between particles and subsequently decreases the apparent density.

Table 4 reports the density properties of the studied systems.

TABLE 4
The fundamental density properties of investigated aluminium alloys

No.	ρ_a [g.cm^{-3}]	ρ_t [g.cm^{-3}]	i [-]	ρ_{th} [g.cm^{-3}]
Al-Mg-Si-Cu-Fe	1.09	1.25	1.15	2.6229
Al-Zn-Mg-Cu-Sn	1.10	3.9	1.23	2.7213

ρ_a is the apparent density, ρ_t is the tap density, i is the ratio ρ_{th}/ρ_a.

Table 5 shows the compressibility behaviour of the investigated systems.

According to data listed in Table 5, the compressibility parameter n is related to the activity of powders to densification by the plastic deformation. In case of powders with high plasticity, n is close to 0.5; in case of low plasticity, n is close to 1. The results show excellent trends for both aluminium alloys. Al-Mg-Si-Cu-Fe alloy (n = 0.5614) shows a higher ability to plastically deform than Al-Zn-Mg-Cu-Sn alloy (n = 0.6599).

TABLE 5
Compressibility parameters of investigated aluminium alloys

No.	Po [%]	K 10^{-2} [-]	n [-]	p_1 [MPa]	r [-]
Al-Mg-Si-Cu-Fe	58.44	11.01	0.5614	57.86	0.9821
Al-Zn-Mg-Cu-Sn	59.58	3.82	0.6599	167.30	0.9943

p_1 represents the fictive pressure.

The effect of powder morphology also reflects in the values of the compressibility parameter K, which is lower for Al-Zn-Mg-Cu-Sn ($K = 3.82 \cdot 10^{-2}$) than for system Al-Mg-Si-Cu-Fe ($K = 11.01 \cdot 10^{-2}$). The difference between the Al-Mg-Si-Cu-Fe and the Al-Zn-Mg-Cu-Sn system is connected to the effect of particle geometry (represented by particle size distribution). It is very important to note that the lubrication of aluminium powder during compaction and ejection has to be considered, since it has a strong tendency to stick to the tooling [27-29].

Fig. 3 shows the relationship between experimental and calculated data according to the aforementioned equations.

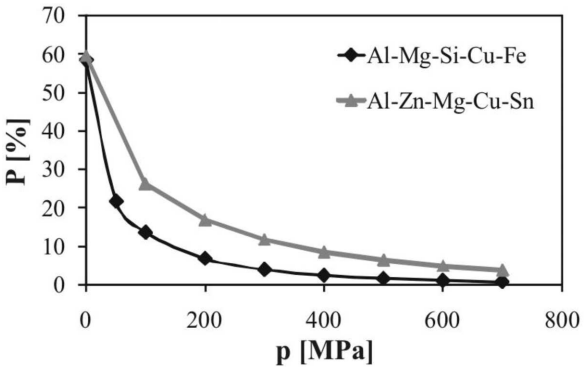

Fig. 3. Compressibility of both aluminium alloy

Compressibility of the Al-Mg-Si-Cu-Fe alloy is slightly higher than that of the Al-Zn-Mg-Cu-Sn alloy, mainly in the area of pressing pressures from 100 to 500 MPa.

The compressibility equation (1) enables to calculate the pressure p_1 needed for achieving almost close to zero porosity, only by particle movements. The results show a shifting from 167.3 MPa (Al-Zn-Mg-Cu-Sn) to 57.86 MPa for Al-Mg-Si-Cu-Fe.

The unetched microstructures after pressing are shown in the following figures.

Fig. 4a, b presents the typical microstructures for low pressures when the densification of the powder occurs by particle rearrangement (translations and rotations of particles) providing a higher packing coordination. Lower pressure creates high volume of porosity. Using low pressure may lead to edge blunting and porosity agglomeration, consequently a low green strength was found. This is clear visible, mainly in the microstructure of Al-Zn-Mg-Cu-Sn alloy.

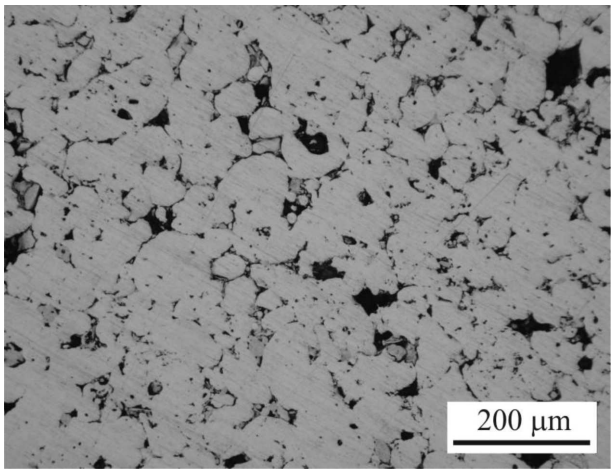

Fig. 4.a Microstructure of aluminium alloys at 50 MPa, Al-Mg-Si-Cu-Fe

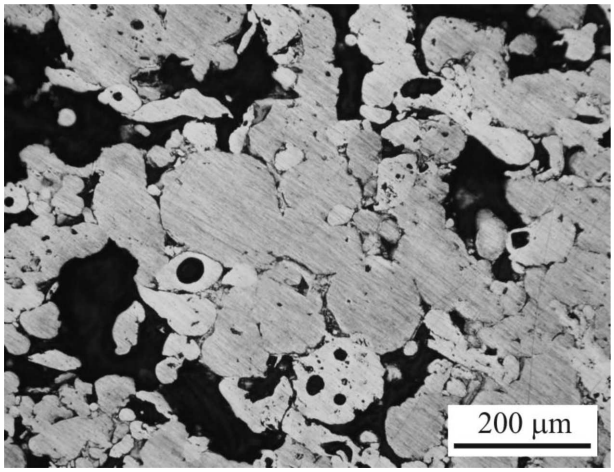

Fig. 4.b Microstructure of aluminium alloys at 50 MPa, Al-Zn-Mg-Cu-Sn

After the finishing of particle rearrangement, the elastic and plastic deformation of particles starts through their contacts. Fig. 5a, b presents the detailed microstructures with small work hardened areas by implication of plastic deformation.

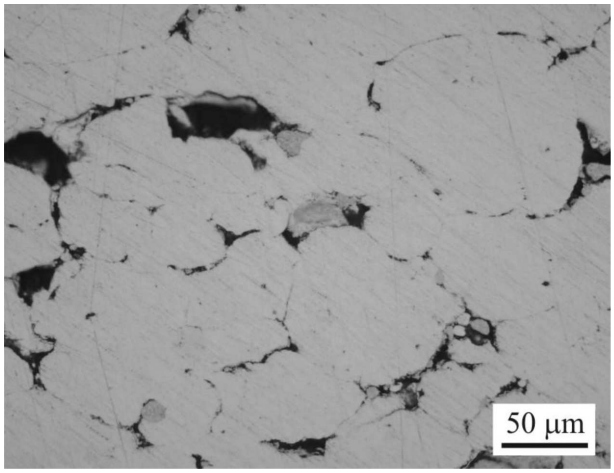

Fig. 5.a Microstructure of aluminium alloys at 200 MPa, Al-Mg-Si-Cu-Fe

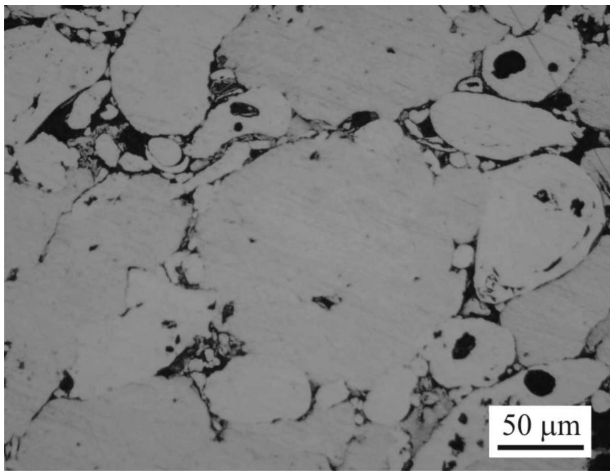

Fig. 5.b Microstructure of aluminium alloys at 200 MPa, Al-Zn-Mg-Cu-Sn

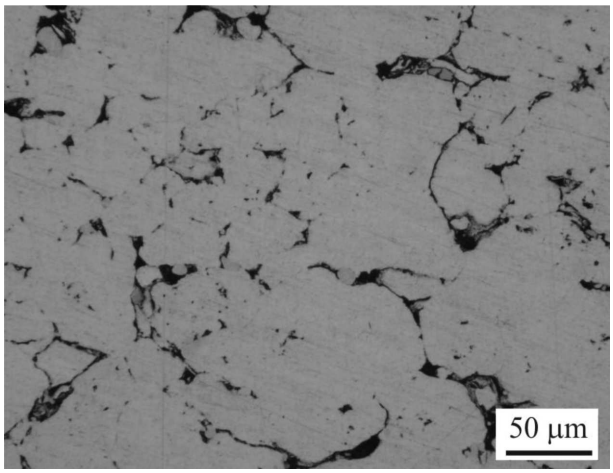

Fig. 6.a Microstructure of aluminium alloys at 400 MPa, Al-Mg-Si-Cu-Fe

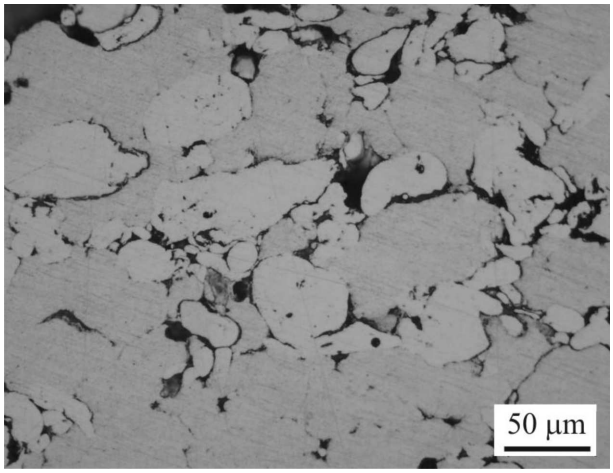

Fig. 6.b Microstructure of aluminium alloys at 400 MPa, Al-Zn-Mg-Cu-Sn

Fig. 6a, b shows that the contact area between the particles increases and particles undergo extensive plastic deformation in both aluminium alloys. During compaction the particles deform following to the formation of solid interfaces at the point or planar particle contacts “compaction facets” [30],

representing areas with elevated free energy. Thus, the potential areas for nucleation and growth of inter-particle necks during the sintering are increased. In terms of compressibility, the pressing pressure of 400 MPa seems to be appropriate for achieving the desirable cold welding.

The final stages of densification of powder particles under the pressure of 600 MPa are presented in Fig. 7a, b (optical microscopy).

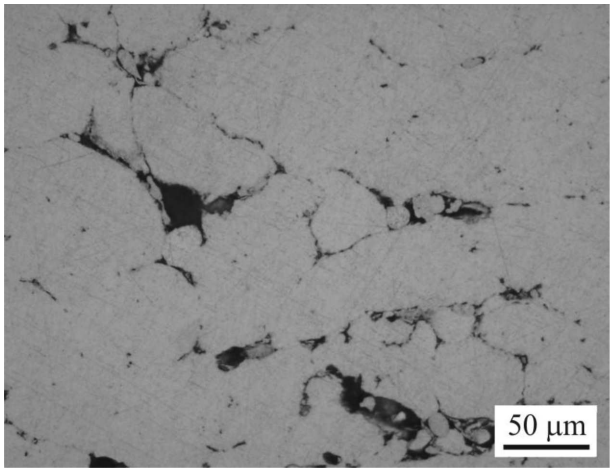

Fig. 7. a Microstructure of aluminium alloys at 600 MPa, Al-Mg-Si-Cu-Fe, Al-Zn-Mg-Cu-Sn, optical microscopy

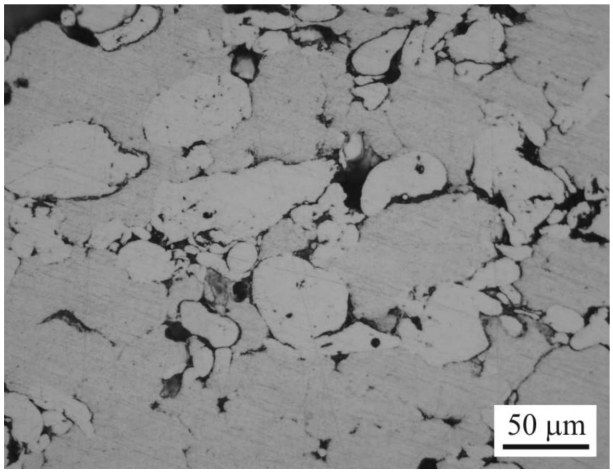

Fig. 7.b Microstructure of aluminium alloys at 600 MPa, Al-Mg-Si-Cu-Fe, Al-Zn-Mg-Cu-Sn, optical microscopy

4. Discussion

It is clear from the results, that the Al-Mg-Si-Cu-Fe system has a cold welding development bigger than the Al-Zn-Mg-Cu-Sn one. This is confirmed by the results of compressibility parameters K and n, as well as microstructure investigation. Compressibility parameters K and n cover the plastic deformation processes performed during pressing as well as those defined by the physical significance. Moreover, they allow to quantify the intensity of the development of compaction facets. The geometrical properties are represented by powder particles shape and distribution (powder particle morphology); since the compressibility parameter K, which is related to powder particles shape and distribution, is difficult to be evaluated directly, the measurement of microhardness values can provide its indication. Plastic properties of powder particles cover the compressibility parameters n in consideration of FEM analysis, as presented in [13]. Therefore, the dimensions of particle contact areas – *compaction facets* – depend primarily on particle shape and the localization of plastic deformation depends on surface geometry and pressure level. This means that the compaction facets, as results of overall compressibility effect, depend on granulometry, compaction pressure, and particle surface roughness form discontinuous adhesive and mechanical particle contacts.

In a number of materials densified by plastic flow, cusp-shaped pores <1 μm in size have been observed. The radius of material on the pore surface is much smaller than the particle radius. The material surrounding the pore has a shape typical of atomized produced powders (Fig. 8a, b). Plastic deformation of powder particles leading to intimate contact between oxide- and/or contamination-free surfaces results in the formation of chemical bonds and adhesion.

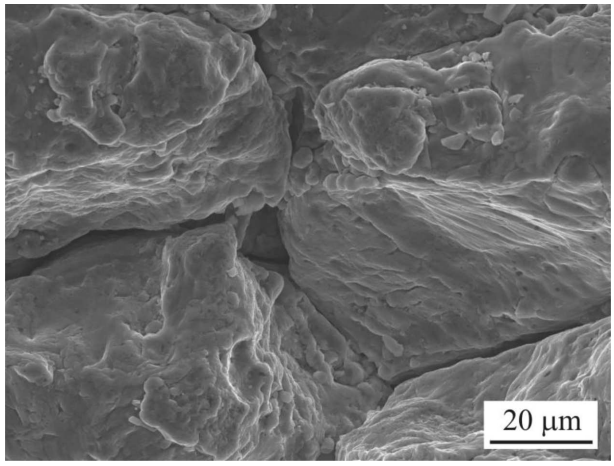

Fig. 8. a Microstructure of aluminium alloys at 600 MPa, Al-Mg-Si-Cu-Fe, Al-Zn-Mg-Cu-Sn, scanning electron microscopy

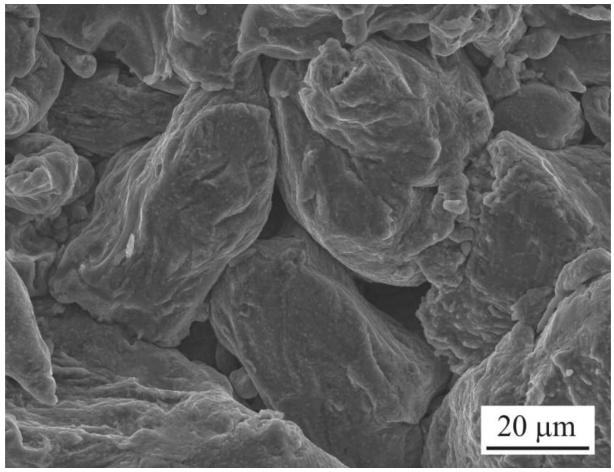

Fig. 8.b Microstructure of aluminium alloys at 600 MPa, Al-Mg-Si-Cu-Fe, Al-Zn-Mg-Cu-Sn, scanning electron microscopy

In terms of porosity, the pore radius decreases with deformation. It means that pressing pressure supported the

porosity closure. Such cusp-shaped pores are less stable under applied pressure than the spherical pores formed by diffusional flow, considered reference [26]. What in principle opposes the closure of cusp-shaped pores is the increasing surface tension force on the concave surfaces, resulting in LaPlace compressive stresses on these surfaces. At very high pressing pressure delaminated (cracking across the particle, Fig. 9) specimens were failing in the investigated systems; this is basically due to the work hardening effect. On the other hand, very low pressure was not able to create sufficient compact. These microstructure examinations correspond to the compressibility results as well as fictive pressure p_1 (167.3 MPa for Al-Zn-Mg-Cu-Sn and 57.86 MPa for Al-Mg-Si-Cu-Fe). These results open the question of "fitness" using the lower pressure for compressibility evaluation. By reason of a proper compressibility parameters is appropriate to use various pressing pressure from lower (50 and 100 MPa) up to higher level (700 MPa). When is possible to find the "boundary" conditions for plastic deformation behaviour of investigated materials, considering that these aforementioned pressing pressure provide a scatter of results, but is necessary to take it in the calculation.

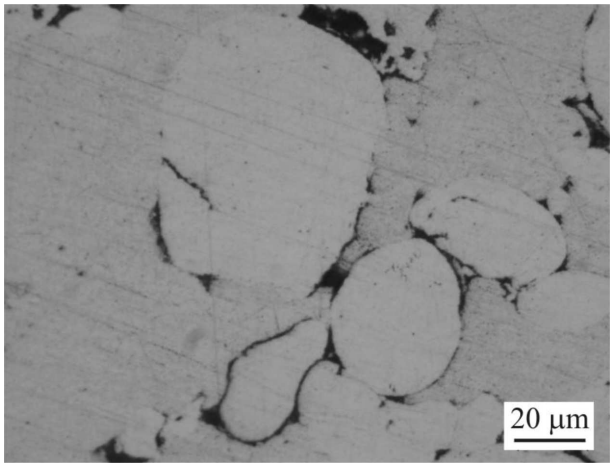

Fig. 9. Microstructure of aluminium alloys Al-Mg-Si-Cu-Fe

5. Conclusion

Considering the densification of metal powders in uniaxial compaction, quantification of aluminium compaction behaviour was studied. The evaluation of compressibility values with pressing pressure enables to characterize the effect of particles geometry and matrix plasticity on the compaction process that is confirmed by microstructure evaluation. The presented results exhibit a high value of plasticity, as a property related to compressibility, and consequently promising compressibility data in terms of industrial potential are obtained.

Acknowledgements

R. Bidulsky thanks the Politecnico di Torino, the Regione Piemonte, and the CRT Foundation for co-funding the fellowship. J. Bidulska thanks Slovak national projects VEGA 1/0385/11.

REFERENCES

[1] J. Bidulska et al., Archives of Metallurgy and Materials **58**, 371-375 (2013).
[2] P. Bazarnik, M. Lewandowska, K.J. Kurzydlowski, Archives of Metallurgy and Materials **58**, 371-375 (2013).
[3] K.S. Dunnett, R.M. Mueller, D.P. Bishop, Journal of Materials Processing Technology **198**, 31-40 (2008).
[4] C.C. Koch, Journal of Materials Science **42**, 1403-1414 (2007).
[5] R.Y. Lapovok, Journal of Materials Science **40**, 341-346 (2005).
[6] X. Wu, W. Xu, K. Xia, Materials Science and Engineering A **493**, 241-245 (2008).
[7] J. Bidulská, T. Kvačkaj, R. Bidulský, M. Actis Grande, T. Donič, M. Martikán, Acta Physica Polonica A **117**, 864-868 (2010).
[8] F. Nový, M. Činčala, P. Kopas, O. Bokůvka, Materials Science and Engineering A **462**, 189-192 (2007).
[9] F. Nový, O. Bokůvka, V. Škorík, Chemicke Listy **105**, s494-s496 (2011).
[10] P. Novak, D. Vojtech, J. Serak, V. Knotek, B. Bartova, Surface and Coatings Technology **201**, 3342-3349 (2006).
[11] P. Novak, D. Vojtech, J. Serak, Surface and Coatings Technology **200**, 5229-5236 (2006).
[12] R. Lapovok, D. Tomus, J. Mang, Y. Estrin, T.C. Lowe, Acta Materialia **57**, 2909-2918 (2009).
[13] V.I. Betekhtin, A.G. Kadomtsev, V. Sklenicka, I. Saxl, Physics of the Solid State **49**, 1874-1877 (2007).
[14] E. Hryha, P. Zubko, E. Dudrová, L. Pešek, S. Bengtsson, Journal of Materials Processing Technology **209**, 2377-2385 (2009).
[15] M. Mihalikova, Metalurgija **49**, 161-164 (2010).
[16] L. Lityńska-Dobrzyńska, J. Dutkiewicz, W. Maziarz, L. Rogal, Journal of Microscopy **237**, 506-510 (2010).
[17] A. Pozdnyakova, A. Giuliani, J. Dutkiewicz, A. Babutsky, A. Chyzhyk, J.A. Roether, F. Rustichelli, M.G. Ortore, Intermetallics **18**, 907-912 (2010).
[18] L. Lityńska-Dobrzyńska, J. Dutkiewicz, W. Maziarz, A. Kanciruk, Journal of Microscopy **236**, 119-122 (2009).
[19] M. Maccarini, R. Bidulský, M. Actis Grande, Acta Metallurgica Slovaca **18**, 69-75 (2012).
[20] T. Kvačkaj, M. Zemko, R. Kočiško, T. Kuskulič, I. Pokorny, M. Besterci, K. Sulleiova, M. Molnarova, A. Kovačova, Kovove Materialy **45**, 249-254 (2007).
[21] M. Matvija et al., Acta Metallurgica Slovaca **18**, 4-12 (2012).
[22] I. Forno, M. Actis Grande, Acta Metallurgica Slovaca **19**, 271-281 (2013).
[23] E. Dudrová, Ľ. Parilák, E. Rudnayová, M. Šlesár, 6^{th} International Conference on PM in ČSSR, Brno, DT ČSVTS Žilina, Part 1, 73-83 (1982).
[24] Ľ. Parilák, E. Dudrová, R. Bidulský, M. Kabátová, Proceedings of Euro PM **4**, Eds. Danninger, H. & Ratzi, R., Wien, EPMA/Shrewsbury, 593-598 (2004).
[25] E. Hryha, E. Dudrova, S. Bengtsson, Powder Metallurgy **51**, 340-342 (2008).

[26] ASM Handbook Vol. 7: Powder Metal Technologies and Applications, ASM International/Warrendale (1998).
[27] W. K e h l, M. B u g a j s k a, H.F. F i s c h m e i s t e r, Powder Metallurgy **26**, 221-227 (1983).
[28] J.H. D u d a s, W.A. D e a n, International Journal of Powder Metallurgy **5**, 21-36 (1969).
[29] L.-P. L e f e b v r e, Y. T h o m a s, B. W h i t e, Journal of Light Metals **2**, 239-246 (2002).
[30] M. S l e s a r, E. D u d r o v a, L. P a r i l a k, M. K a b a t o v a, Science of Sintering **32**, 83-96 (2000).

Received: 15 February 2013.